AIMS Materials Science, 4(5): 1186-1201.
DOI: 10.3934/matersci.2017.5.1186
Received: 16 July 2017
Accepted: 11 September 2017
Published: 13 November 2017

http://www.aimspress.com/journal/Materials

Research article

Preparation of valuable products from cleaned carbon of fuel ash

Mahmoud A. Rabah [1,*], Mohamed B. El Anadolly [2], Rabab A. El Shereif [2], Mohamed Sh. Atrees [3], and Hayat M. El Agamy [3]

[1] Chemical and electrochemical lab., Mineral Processing Dept. Central Metallurgical Research and Development Institute, P.O.Box 87, Helwan Cairo, Egypt
[2] Department of Chemistry, Faculty of Science, Cairo University, Egypt
[3] Nuclear materials Authority, El Malady Cairo, Egypt

* **Correspondence:** Email: mrabah010@gmail.com; mahmoud.rabah@ymail.com.

Abstract: This work provides a method to use waste carbon of fuel ash left after steam generation in power stations in Egypt to prepare valuable products such as activated carbon and alumina-dolomite-carbon bricks. Carbon content in ash as received amounts to 41.22%, S to 7.2% and others to 11.36% compared to 80%, 4.2% and 2.55% after cleaning respectively. Impurities (21 wt%) in carbon were decreased to 4.78% by sulphuric acid leaching, and carbon content in ash amounts to 95.22%, S to 4.35% and others to 0.36%. Activated carbon (AC) with surface area of 1050 m^2/g was prepared by steam gasification at ≤800 °C in presence of zinc chloride. The activation process has ΔE value of 82.6 kJ/mol. The AC quality was tested by adsorption of hexa-valent Cr^{6+} from waste tannery solution. It adsorbed 124 mg Cr^{6+}/g C equivalent to 94% of the present Cr^{6+}. Alumina-dolomite-carbon bricks were made by hot mixing Al_2O_3, dolomite, C with coal tar pitch. The green bricks were baked at 1000 ℃, multi-impregnated with molten coal tar pitch followed by charring at 750 ℃ to seal the porous system of the fired bricks.The prepared brick samples have high density value, good thermal and chemical stability, an outstanding resistance against hydration (>60 days). Brick body is a heterogeneous composite of dolomite and carbon particles that possess different physico-chemical properties.

Keywords: fuel ash; active carbon; alumina-dolomite-carbon bricks; steam gasification

1. Introduction

Fossile fueloil is used in Egypt providing close to 90% of entire power needs. Upon combustion of the oil, it produces fly and bottom ashes. Water used in electricity generating plants is supplied from River Nile. Assiut electric power plant has 2 generation units 312 MWh each (a maximum power of 2 × 312MW/h) [1]. Solid wastes from power plants can be classified into three categories. Partial utilization of ash has been commonly practiced, as fill for roads, runways, construction sites—cement and brick admixtures. Burning heavy fuel oil yields about 3 kilogram of ash per cubic meter of oil [2], whereby most of the remaining was ash (approximately 90%). In some cases, ash may be collected by electrostatic precipitators or cyclones [3,4]. It has been reported that some ashes from the flue-gas and boiler residue were fed to the agriculture growing area to reclaim the soil. The minerals in ashes may improve or increase the land fertility, crop growth and yield more agriculture productivity [2].

Fuel oil ash may contain vanadium and other noncombustible and potentially toxic chemicals that may be present in the oil [5,6]. The recovery methods of vanadium from the vanadium-containing ashes showed that there was no single approach to directly recovering vanadium. Specific leaching mode from each ash depended on its chemical and phase compositions [7]. The type of fuel determines the amount and properties of ash. For instance, coal used in boiler produced large amount of both types of ashes, whereas fuel oil produces little bottom ash. On the other hand, gas produces little of either the two types of ashes. U.S. Geological Survey reported that fossil fuel combustion resulted in concentration of most trace elements in ash by approximately 10 times the concentration in the original fuel [8,9] Heavy oil ash (HOFA) consisted of inorganic substances such as silicon dioxide (SiO_2), iron oxide (Fe_2O_3), aluminum oxide (Al_2O_3) and 70–80% unburned carbon [10] The HOFA contains a considerable amount of metal values such as vanadium (V, 20–30%), nickel (Ni, 0.8–6%), arsenic (As), cadmium (Cd), mercury (Hg), chromium (Cr) and copper (Cu) [11]). Worldwide several million tons of HOFA are generated each year, and only a small portion of these ashes is re-used for productive purposes [12].

Recently, recycling concern of ash is due to increasing landfill costs and current interest in sustainable development. In U.S., coal-fired power plants generate ≥71 million tons of ash [13]. In case about 42 million tons of the ash is recycled, the need for landfill space will be only 27,500 acres. Other environmental benefits to recycling ash includes reducing the demand for virgin materials that would need quarrying and cheap substitution for materials such as Portland cement [13,14]. As of 2006, about 125 million tons of coal-combustion byproducts, including ash, were produced in the U.S. each year, with about 43% of that amount used in commercial applications, according to the American Coal Ash Association Web site. As of early 2008, the United States Environmental Protection Agency hoped that figure would increase to 50% [14].

The aim of the present work is to reuse fuel ash to prepare valuable products such as activated carbon and alumina-dolomite-carbon bricks. The impurities in ash amounts to 21 wt% were decreased to 4.78 % by leaching with sulphuric acid. Carbon increased to 95.22%, S to 4.35% and impurities to 0.36%. Activated carbon (AC) having surface area of 1050 m^2/g pores of meso size was prepared by steam gasification at 900 ℃. The effect of mass ratio of water vapour:carbon on the quality of the produced activated carbon was investigated. Also it shows that leaching of the ash with

sulphuric acid has no harmful effect on the thermal and mechanical properties of the prepared bricks samples.

The objectives are:

1. To treat the waste ash by leaching with sulphuric acid to remove the major part of its impurities mainly of mineral source.
2. To prepare active carbon by steam gasification at temperature ≤1000 °C for time up to 90 minutes.
3. To prepare alumina-dolomite-carbon bricks by mixing alumina, dolomite and purified carbon and use of coal tar pitch as a binding agent.
4. To improve the thermal and mechanical stability of the fired bricks by multi impregnation using coal tar pitch. Each impregnated sample was claimed at 750 ℃ to carbonize the tar pitch.
5. To predict that the method is effective, simple and friendly environmental.

2. Materials and Method

2.1. Materials

Ash sample weighing about 10 kg was supplied by Assuit Power station plant 2 × 312 MW (East of Assuit City). The sample was dried, fine ground, and sieved to pass an opening size 42 μm prior to de-ashing. It was washed with distilled water in hot conditions for 3 hours.

2.2. Characterizxation of Ash

2.2.1. Chemical Analysis

Chemical analysis of a sample was carried out according to American Society for Testing and Materials method ASTM, D1762-84. Samples were dried for 3 h at 105 ℃ to get rid of moisture before analysis. Volatile matters analyses was carried out at 550 ℃ for 7 min in capped crucibles while ash content was determined at 900 ℃ for 6 h in open crucibles. Carbon content was determined by difference as shown in Equation (3). The ash content is defined as the remaining inorganic contents after the complete removal of fixed carbon, volatile matter and moisture. Sulphur was determined by the Eschka method as lead sulphate.

The ash content was calculated using the equation:

$$\text{Ash } [\%] = \frac{\text{ash weight [g]}}{\text{oven dry weight of ash sample [g]}} \times 100\% \quad (1)$$

Volatile matters were calculated using the equation:

$$\text{Volatile matter (VM) } [\%] = \frac{\text{weight of volatile compound [g]}}{\text{oven dry weight of ash sample [g]}} \times 100\% \quad (2)$$

$$\text{Fixed Carbon (FC) } [\%] = 100\% - (\text{VM} + \text{Ash}) \quad (3)$$

2.2.2. Elements Content

Determination of carbon (C), hydrogen (H), nitrogen (N), and sulfur (S) was conducted using a Costech TM. Elemental Analyzer, ECS 4010 Elemental Combustion System.

2.2.3. Particle Size Distribution

Representative sample was placed into a size screen analyzer (Retsch S1000) to determine the size distributions of particles.

The BET surface area and pore volume distribution of the obtained carbon were determined using Micromeritics ASAP 2020 using nitrogen adsorption isotherms at 77.35 K. A sample of 0.3210 g was degassed and dried at 150 ℃ under vacuum for 6 h [15].

2.2.4. X-ray Fluorescence Spectroscopy Determination (XRF)

Quantitative analysis of the major elements within the candidate CFA with particle size less than 99 μm (obtained by sieving) was determined by X-ray Fluorescence Spectroscopy, using a Magi"X Pro XRF spectrometer from PANalytical. The sample was placed in an aluminum cup and hydraulically pressed into pellets under very high pressure of 20.2 MPa for 60 seconds.

2.2.5 Scanning Electron Microscope (SEM)

To examine the surface morphology of samples was observed by *JEOL JSM*-646LV Scanning Electron Microscope. The sample was initially dried, fixed with double-side masking tape, and then gold-coated using a sputtering machine for 6 minutes in order to improve the conductivity of the sample. The aim of carrying out this test was to determine the shape of the carbon particles.

2.2.6. Fourier Transform Infrared Spectroscopy (FT-IR)

The functional groups on the surface of the OFA were analyzed using FPC FTIR Perkin Elmer spectrophotometer. A weight of 1–2 mg of the OFA was mixed thoroughly with 1.0 g of fine dried powder of KBr. Then the resulting mixture was hydraulically pressed at10 ton/m^2 to obtain a thin transparent disk. The thin disk was placed in an oven at 110 ℃ for 4 hours to prevent any interference of any existing water vapor or carbon dioxide molecules. All the FTIR spectra were taken in the transmission mode.

2.2.7. Thermal Analysis

Thermal characteristics were determined using a TGA Instrument TGA-50/50H Shimadzu thermogravimetric analyzer. Approximately 10 mg of the sample was heated from room temperature to 1000 ℃ at a heating rate of 10 ℃/min. The thermogravimetric (TG) plots describe the weight loss

of the sample with increasing temperatures while the differential thermogravimetric (DTG) plot illustrates the derivative of sample mass with time at a specific temperature.

2.2.8. Steam Activation

The steam activation process was conducted in a tube furnace fitted with digital temperature control, by inserting superheated dry steam in a tube furnace containing a dish loaded with 10 g de-ashed carbon. The flow rate of steam, temperature and time of steaming were managed to achieve a total loss in weight of 70% max. Figure 1 and Figure 2 show a schematic diagram and a photograph of the test rig used for streaming the carbon respectively.

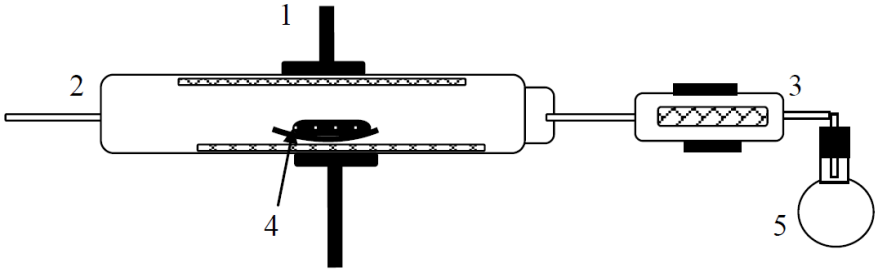

Figure 1. A schematic diagram of the steaming test rig. 1: support, 2: tube furnace fitted with digital temperature control, 3: Steam super heater, 4: Alumina boat with carbon sample, 5: Steam generator.

Figure 2. A Photograph of the experimental rig used to activate carbon.

2.3. Preparation of the Alumina-dolomite-carbon Brick

Alumina-dolomite-carbon bricks were prepared by mixing fines of high quality bauxite, magnesium oxide with carbon up to a weight ratio of 75% of Al_2O_3 and MgO. The blend moistened and bound with fire clay or hot mixed with coal tar pitch and pressed in a rectangular die having the dimensions 100 × 80 × 80 mm. The pressed green bricks, with fire clay, were air-dried for 48 hour and in a drier maintained at 105 ℃ for 24 hours. The bricks were then fired in a salamander crucible. The bricks were covered with graphite powder and covered with a SiC lid. It was then placed in a chamber furnace. The furnace was then switched on and heated at temperature up to 1200 ℃ at a heating rate of 5 ℃/min. The fired bricks were tested for density, chemical and thermal resistance applying the methods given in the standard methods.

2.4. Characterization of Alumina-dolomite-carbon Bricks

Density value was determined with the help of water displacement technique using density bottle 50 ml volume. Mechanical strength was measured by subjection cubes of the brick specimen on a bed plate of a compression machine till rapture.

3. Results and Discussion

3.1. Ash

3.1.1. Chemical Analysis

Ash sample was analyzed to identify the unwanted elements other than carbonto clean it. The major impurity was iron, vanadium and sulphur. Iron and vanadium were successfully leached with 2 M hot sulphuric acid. Only sulphur in sulphidic form was removed while organic sulphur still remains. Table 1 shows the chemical analysis of the ash sample, Table 2 shows the elements detected after acid leaching, while Table 3 shows the elements in the ash after carrying out the acid leaching process. It is seen that the carbon percentage in ash increases from 41% to about 80% by weight.

Table 1. Chemical analysis of the ash sample (as received).

Moisture content (wt%)	Fixed carbon (wt%)	Volatile matter (wt%)	Ash content (wt%)
0–11	≈40	≤28	21.12

Table 2. Elements detected in the fuel ash sample.

C (wt%)	H (wt%)	N (wt%)	S (wt%)
41	0.57	0.59	7.96

Table 3. The XRF analysis of the carbon material.

Components	Amount (%)
S	7.2
Fe	4.7
V	3.14
Ni	2.18
Si	1.00
Ca	1.3
Al	0.314
Zn	0.281
Mg	0.314
Pb	0.204
Ba	0.103
K	0.0985
Cr	0.0979
Ti	0.0589
Mn	0.0405
Sr	0.0398
Co	0.0377
Cu	0.0202
Ir	0.0106
W	0.0103
Sn	0.00545
C	79.8
Total other than C	21.12

3.1.2. Size Distribution

The cumulative particle size of the ash sample is shown in Figure 3. It can be seen that the largest size amounts to 117 μm whereas the finest amounts to 0.09–0.11 μm. The weight percent of these two ultimate sizes amounts to 0.01% and 0.04%. The results given in Figure 3 illustrates that the cumulative weight of the different grain sizes increases to 30% gradually with increase of the grain size up to 10 μm. The cumulative % weight increases dramatically up to 70% with coarser size. With the coarsest size, the cumulative percentage decreases drastically to 100%.

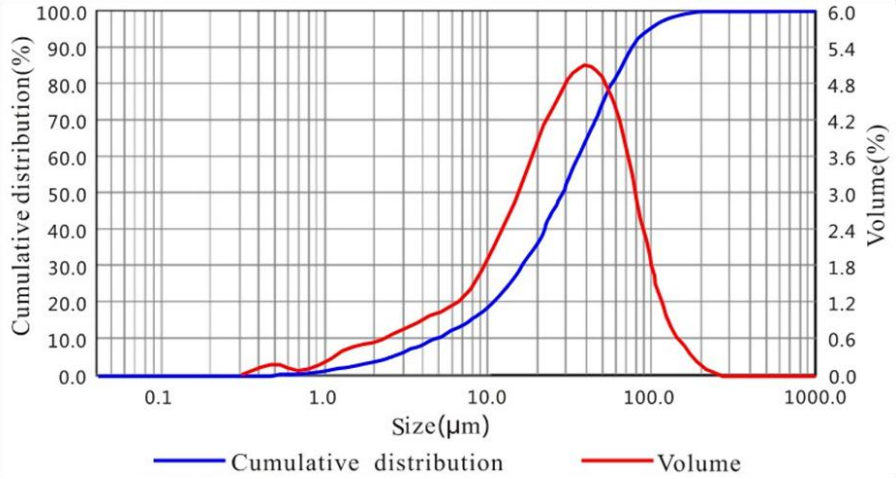

Figure 3. The cumulative weight of the different grain sizes.

The difference in grain size distribution can be explained due to the following reasons:

a. The power plants work in different conditions.

b. The properties of the used fuel may differ, i.e., heavy oil containing excessive weight of free carbon particles generates large amounts of ash as compared to the light fuel.

c. The size of nozzle of the burner fitted in the boiler of the power generation cannot be resist frequent wear [16], showed that carbon in ash may be attributed to modification of the combustion process but there are a number of other factors such as boiler design, boiler operation and fuel properties which also play a part. It is usual that the term loss on Ignition (LOI) is wrongly used to mean chemically investigated analysis. But it is true that in many cases the figures are quite similar, LOI also contains losses which are not carbon and so it is not a true indicator of the ability of a LNB system to burn coal efficiently. In most instances the LOI figure will be marginally higher than CIA depending upon the coal type and sample condition. Refs [17,18] showed that the nozzle geometry plays a vital role in fuel–air mixing. The emission levels of hydrocarbon and NO_x are appreciably reduced with the addition of CON.

d. The air:fuel mass ratios also display an important reason to determine the extent and size of the ash carbon. Air in excess will alleviate the extent on grain size of the formed ash, whereas shortage of in air:fuel mass ration will help smoking of the fuel due to incomplete combustion. Refs [17,19] showed postulated two systems to explore the mechanism of combustion of the mazout fuel. The authors found appropriate method, which would detect change in the composition of the fuel being burned. We have utilized wavelet transform of a signal corresponding to flame radiation intensity. The signal is obtained through flame monitoring system that was developed at Dept. of Electronics, Lublin Univ. of Technology. The multichannel, fiber-optic probe, which is the key part of the system, enables far better spatial resolution of measurements comparing with the other solutions and is specially designed to work in harsh conditions. The two systems were the fiber-optic flame monitoring system and the Wavelet transform system. In conclusion, they reported that both continuous and discrete wavelet transforms are the proper methods, which applied in analyzing flame pulsation signals could detect the change of the fuel to be burned. However, continuous wavelet transform is only applicable at preliminary research for it requires far more computational power.

Results obtained in such a way are more legible. Continuous wavelet transform could be helpful with choosing the proper analyzing wavelet to ensure the desired resolution in time and frequency [scale] domain and avoid phase distortions due to asymmetries of some wavelets. Table 1 shows the approximate analysis of the ash. Table 2 shows the elements present in the ash.

The presence of moisture content in the ash denotes its hygroscopic nature. Volatile matters are due to incomplete combustion in the burner of the power plant, while the extraordinary high percentage of ash content is due to the fact that the oil used is inferior and contains high mineral impurities.

3.1.3. Elemental Analysis

Results obtained assume that the process of combustion taking place in the power station is incomplete. However, burning of the liquid fuel may proceed through a multistep process. The liquid fuel transforms from the liquid phase to a gaseous phase, the latter admixes with the gaseous oxidizer which is air. The gaseous mixture [fuel and air] catches fire. Step (1) involves the presence of fuel mazout in low viscosity to help smooth flow. The latent heat to accomplish this step is comparatively low in summer days and becomes of consideration in winter season of ≈11 kJ/kg ·℃ [20]. The second step involves vaporization of the liquid fuel to a vapor state (1100 kJ/kg/℃), the third step is assigned to transfer the vapor to gas by a latent heat of gas formation, the fourth step in which fuel gas is mixed with air can be physically matched with a very low energy, the fifth step is the burning process of the fuel/air mixture. In the latter step, complete burning of the fuel/air mixture takes place with generation of heat energy and subsequent formation of ash (mainly metallic ash). The overall process of combustion steps 2 through 6, the products are heat energy, carbon, ash and volatiles. This model explains why the ash contains carbon and ash. Table 3 shows the metal components of the carbon material as obtained by XRF determination. The element sulphur is present as organic sulfur, elemental sulfur and pyritic sulfur compounds [21]. Acid leaching removes most of minerals together with some sulphur. This statement finds support from the fact that during carbon activation by steam, the output products contains hydrogen sulphide gas.

3.1.4. The Relation between Surface Area and Pore Size Distribution

Results of surface area and pore size were conducted by BET method using liquid nitrogen. The shape of the curve obtained exhibits a parabolic shape. The optimum value of surface area takes place at 70% amounts to 1050 m^2/g using steam:C ratio of 10. With lower or higher mass ratio, the surface area acquires lower value. The reason of that criteria is that with higher steam:C ratio, the formed pore system collapse and the wall separating two adjacent pores is consumed to form one wider pore. With lower mass ratio less pores are formed.

3.1.5. The Thermo Gravimetric Study

A thermo gravimetric study on the as-received ash sample was carried out. The curve (Figure not given) displays two loss phases. The first phase of loss takes place within the temperature range

25–120 ℃. Such loss in weight is due to the escape of residual moisture content. The second phase takes place at up to 800 ℃. This assumption finds support from the TGA curve and the FT-IR peak appeared at 1631 cm^{-1}, the second phase of loss takes place within the temperature range 450 ℃ to ≈785 ℃ is due to the thermal decomposition and volatilization of the organic compounds found attached to the carbon surface of the ash. The continuous and gradual decrease in weight taking place throughout this temperature range (450–780 ℃) denotes that more than one organic compound on the carbon surface decompose and volatilize at different temperatures. The organic compounds are completely decomposed at 780 ℃.

Results are in a good agreement with the hypothesis reported by Engineeringtoolbox.com [22] and others [23,24].

Figure 4 is a hypothetical schematic structure of carbon particle with metal impurities before and after dashing.

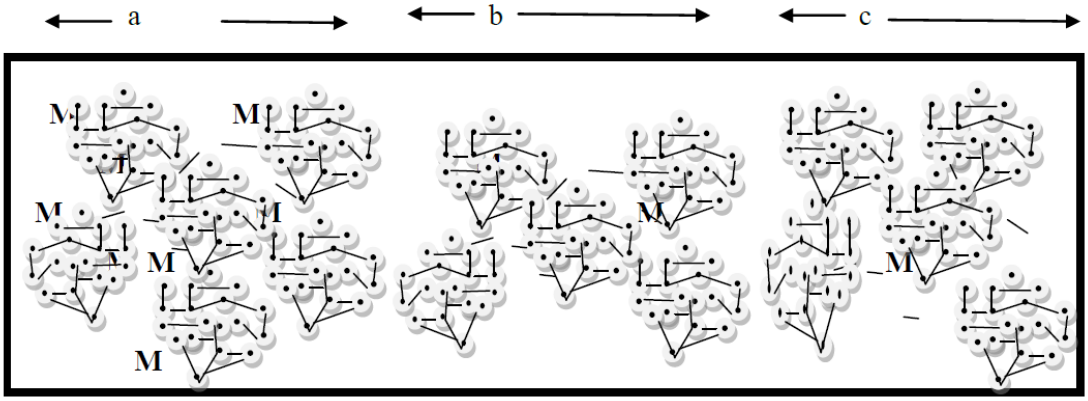

Figure 4. A hypothetical schematic structure of carbon particle with metal impurities before and after dashing. a: Fuel ash composition model, b: Partially deashed carbon entities, c: deashed carbon (M = metal).

3.2. Activation of Cleaned Carbon Derived from the Ash

Preparation of activated carbon was carried out by steam gasification. The test rig used in this process is given in Figure 2. The temperature of activation was taken at 750–950 ℃. Activation process was carried out for different periods up to 90 min. The weight loss of carbon is found insignificant after 45 min. It increases linearly with further increase in time of activation up to 90 min whereby a weight loss amounts to 75%.

Figure 5 shows the effect weight ratio of steam/carbon on the surface area of the obtained activated carbon. It is seen that the curves display an inverted parabolic shape with its optima at 10 mg steam/g carbon. The optimum magnitude of surface area of 1050 m^2/g was displayed at 900 ℃ with steam:carbon weight ratio of 10. With lower of higher steam ratio, the magnitude of surface area displays a lower value. Results can be ascribed to the following model. The carbon obtained after acid leaching of the ash is built up of carbon entities without symmetric ordering of structure, orientation or arrangement. The ash impurities are linked to carbon via bonding of a

covalent magnitude. Carbon loaded with metals has low magnitude of surface area as the metals have very low surface area. Acid leaching removes the metals from carbon that helps to acquires high surface area upon gasification. Although the surface area of the activated carbon obtained from the ash carbon is lower than that of the surface area of carbon prepared from coconut shell, yet it can be considered a convenient quality on basis of cost.

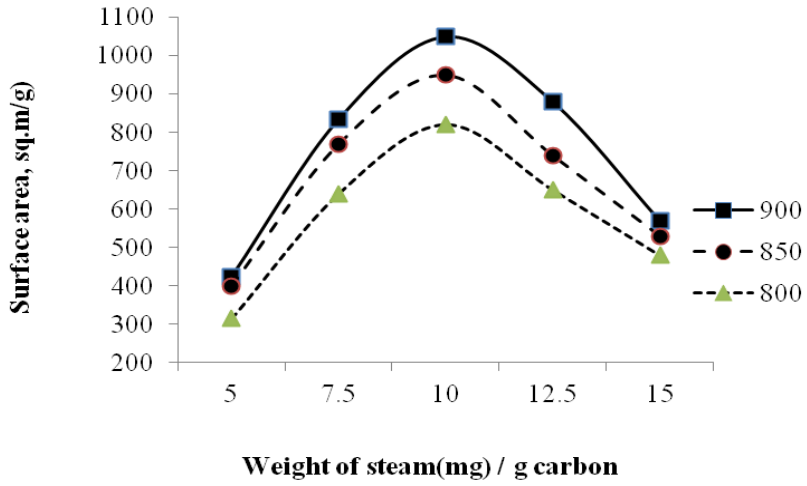

Figure 5. Surface area of carbon as a function of weight of steam:C.

Figure 6 shows the pore volume as a function of size distribution of the obtained activated carbon. It is seen that the meso pores (2–50 μm) exhibits the major volume (58%). Figure 7 shows the Arrhenius plot of the activation process. The ΔE magnitude was computed and found to be 82.6 kJ/mol. Activated carbon sample was tested to adsorb Mg^{2+} and Cr^{6+} from waste Tannery solution.

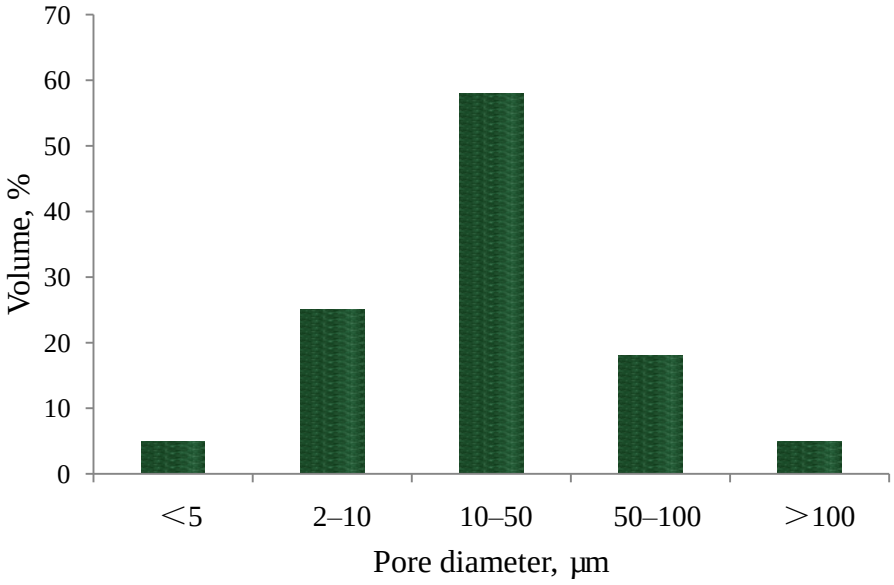

Figure 6. The pore size distribution of the activated carbon prepared from fuel ash carbon.

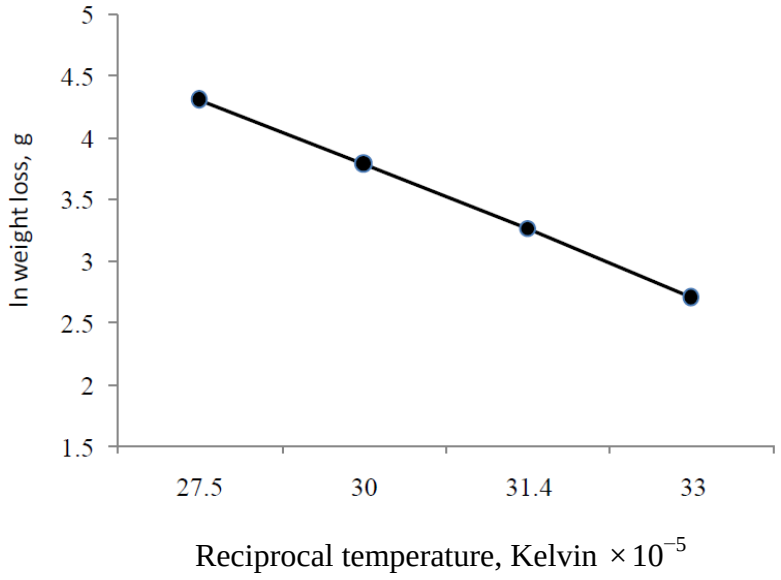

Figure 7. The Arrhenius plot of the activation process.

Results are in a good agreement with model suggested for the mechanism of activation (item 3.6). During thermal heating of the carbon under superheated steam, certain sites on the carbon surface get overheated and these constitute the most active points of reaction with steam. At these sites, initiation of pore entrance starts. With time the pore system develops and a porous structure develops. It follows that the surface area of the activated carbon increases with the increase in pore system. With more time or at higher temperatures ≥950 ℃, some walls separating two adjacent pores are consumed in the steam–C reaction and a new pores with wider diameter initiate leading to a decrease in the surface area of the carbon. The surface area of a wide pore is comparatively less than two adjacent pores having lower diameter. Figure 8 shows the SEM investigation of the activated carbon.

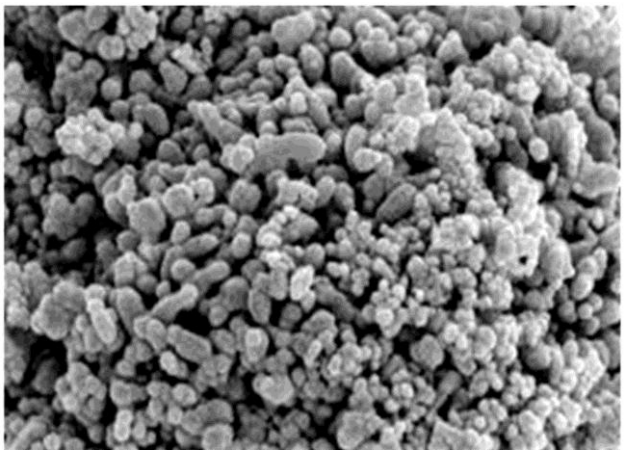

Figure 8. The SEM of active carbon prepared from cleaned waste fuel carbon.

Figure 9 shows that the extent of adsorption increases with the increase of the mass of activated carbon used for adsorption. Nearly adsorption of the all the chromium ions are adsorbed with 50 g carbon/one liter of the waste solution.

It is also seen that about 124 mg CR^{6+} were adsorbed by 1 g carbon corresponding to 94% of the available chromium ions in waste tannery solution.

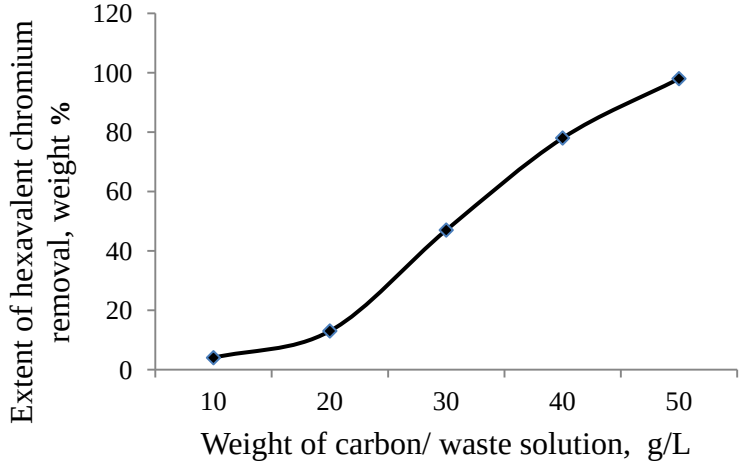

Figure 9. The extent of chromium adsorption from waste tannery solution as a function of the weight of activated carbon at room temperature.

3.3. The Alumina-dolomite-carbon Bricks

Brick body is a heterogeneous composite body. Results of density measurement of the finished brick sample revealed that the density value increases with the increase in the alumina content and decreases with the increase of dolomite. The green brick samples are stronger than the baked bricks. In practice, for ladle furnace (LF) needs, the CCS of high performance green and baked carbon-bonded dolomite bricks amounts to 500 kg/cm^2 and 450 kg/cm^2 respectively. The prepared samples acquired CCS values close to or higher than those of commercial quality. The bricks mechanical strengths were traced as a function of binder content. It was shown that this property increased with increase in bider content attaining its maximum with 6–8% by weight of the bonder. Results can be explained by the gradual satisfaction of body voids with a carbon framework left after charring of the binder. Voids is only satisfied with an adequate carbon framework with >9 wt% binder. With lower binder content, the porous system of the brick body is not fully filled in. Figure 10 shows the mechanical breaking strength (MBS) of the samples. It can be seen that the mechanical strength is directly related to the mass percentage of alumina present in the body of the brick. The maximum breaking strength MBS amounts to 325 kg/cm^2 whereas the minimum value amounts to 180 kg/cm^2. Results can be ascribed to the fact that the filling particles of the brick are bound with hard carbon bridges formed by thermal charring of the coal tar pitch that was used as a binding agent. Impregnation also imparts a support parameter to the mechanical properties of the brick body.

Alumina is a high refractory material with high hardness property as compared to both magnesium oxide and carbon.

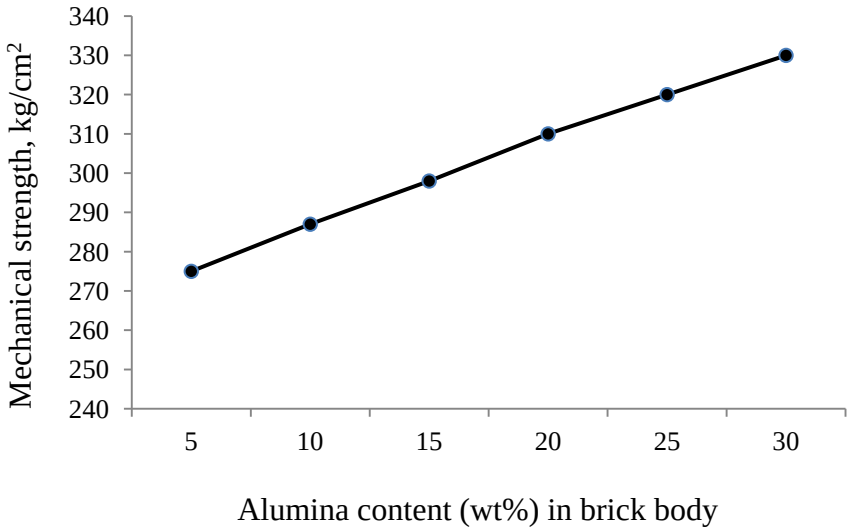

Figure 10. The mechanical strength of the fired brick as a function of alumina content.

4. Conclusion

From the above results, it can be concluded that ash contains different elements tabulated in Tables 1 and 3. The weight percent of free carbon amounts to 40%. Total ash amounts to 21%, ash contains iron oxide (4.7%), vanadium and nickel (3.14 and 2.18%). The detection of total sulphur in high percentage (7.2%) makes the carbonaceous material immaterial for application otherwise it is removed. The work done improves the physic-chemical properties of the separated carbon to meet the specifications for the preparation of different engineering materials such as activated carbon (adsorbent for purification of wastewater in galvanization industry, printing of electronic boards, deionizing of drinking pevarage water, decolorization of sxectra pure water, recovery of metals ions from solutions recovery of chloride and fluoride ions from brakish water, separation of poisoning soluble gases, adsorption of poisoning gases from aor during dirty war, etc…) and alumina-dolomite-carbon bricks for use in steel furnaces, and other useful products (alumina-dolomite-carbon bricks for use in steel furnaces, lining of ladle furnaces, lining of chemical corrosive containers and other useful products. The method of treatment is rather simple and cost effective.

Conflict of Interest

All authors declare no conflicts of interest in this paper. This is to state that the nuclear materials Authority is of interest. This study was not funded by any authority, the first author has not received research grants from CMRDI. The second and third authors have not received a speaker honorarium and do not own stock in the Cairo University. Author #4 is a member of committee of the Nuclear materials Authority.

References

1. Bady MF, Hassanien HM, El-Deen AK, et al. (2011) Study of solid waste and ashes content of radioactive and heavy metals in assiut thermal power plant. *J Eng Sci Assiut Univ* 39: 1335–1342.
2. Tsai SL, Tsai MS (1997) Study on the physical and chemical characteristics, yield and TCLP test of oil-fired fly ash. *Min Metall* 41: 57–68.
3. Hsieh YM, Tsai MS (2003) Physical and chemical analyses of unburned carbon from oil-fired fly ash. *Carbon* 41: 2317–2324.
4. Ng WJ, Jern NW (2006) *Industrial Waste Treatment*, London: Imperial College Press.
5. Harza Consulting Engineers and Scientists (1994) Water Quality Improvement and Conservation Project. Submitted to: United States Agency for International Development, Amman Chamber of Industry, Ministry of Water and Irrigation, Jordan.
6. Doty S, Turner CW (2004) *Energy management handbook*, Lilburn: The Fairmont Press, Inc.
7. Clean Air Task Force, the Land and Water Fund of the Rockies, The Last Straw: Water Use by Power Plants in the Arid West, the Energy Foundation, the Hewlett Foundation, USA, 2003. Available from: http://www.lawfund.org/ and http://www.catf.us/.
8. Tsygankova MV, Bukin VI, Lysakova EI, et al. (2011) The recovery of vanadium from ash obtained during the combustion of fuel oil at thermal power stations. *Russ J Non-ferrous Metals* 52: 19–23. Original Russian Text ©, published in Izvestiya VUZ. Tsvetnaya Metallurgiya, 2011, 1: 21–26.
9. Zielinski RA, Finkelman RB (1997) Radioactive elements in coal and fly ash: abundance, forms, and environmental significance. US Geological Survey.
10. Saeedi M, Rezaei Bazkiaei A (2008) Characterization of thermal power plant fuel oil combustion residue. *Res J Environ Sci* 2: 116–123.
11. Kwon WT, Kim DH, Kim YP (2004) Characterization of heavy oil ash generated from a power plant. *ATM* 6: 260–263.
12. Mofarrah A, Husain T, Danish EY (2011) Investigation of the potential use of heavy oil fly ash as stabilized fill material for construction. *J Mater Civil Eng* 24: 684–690.
13. Mõtlep R, Sild T, Puura E, et al. (2010) Composition, diagenetic transformation and alkalinity potential of oil shale ash sediments. *J Hazard Mater* 184: 567–573.
14. American Coal Ash Association (2005) CCP Production and Use Survey.
15. McCabe R (2008) Above ground, a golf course. Just beneath it, potential health risks. The Virginian-Pilot.
16. Gregg SJ, Sing KSW (1982) *Adsorption, Surface Area and Porosity*, London: Academic Press.
17. Vairamuthu G, Sundarapandian S, Kailasanathan C, et al. (2016) Experimental investigation on the effects of cerium oxide nanoparticle on Calophyllum inophyllum (Punnai) biodiesel blended with diesel fuel in DI diesel engine modified by nozzle geometry. *J Energy Inst* 89: 668–682.
18. Thompson AW (1997) A burner manufacturer's approach to tackling carbon in ash.
19. Wójcik WW, Kotyra A, Duk M, et al. (2003) The Fibre-Optic System Detecting the Burning Mazout in Power Boilers. *Elektronika ir Elektrotechnika* 49.

20. Elektronika IR elektrotechnika (2003) Nr. 7(49) T 191 Aukstuju Dazniu Technologija Mikrobongos.
21. Shepherd M (1985) Electric Power Research Institure Jourml.
22. Engineeringtoolbox, Tools and Basic Information for Engineering and Design of Technical Applications, 2015. Available from: https://www.engineeringtoolbox.com/.
23. Lozano LJ, Juan D (2001) Solvent extraction of polyvanadates from sulphate solutions by primene 81R. Its application to the recovery of vanadium from spent sulphuric acid catalysts leaching solutions. *Solvent Extr Ion Exc* 19: 659–676
24. Khan AA, De Jong W, Jansens PJ, et al. (2009) Biomass combustion in fluidized bed boilers: Potential problems and remedies. *Fuel Process Technol* 90: 21–50.

AIMS Press